Quantum bistability and spin current shot noise of a single quantum dot coupled to an optical microcavity

Ivana Djuric, Marko Zivkovic, Chris P. Search, and Greg Recine
Department of Physics and Engineering Physics, Stevens Institute of Technology, Hoboken, New Jersey 07030, USA
(Received 15 July 2008; published 19 November 2008)

Here we explore the quantum-mechanical limit of bistability that appears in the spin-dependent transport through a single quantum dot coupled to an optical microcavity. The spin current is generated by electron tunneling between a single doped reservoir and the dot combined with intradot spin-flip transitions induced by a quantized cavity mode. Earlier research has shown that in the classical limit where a large number of such dots interacts with the cavity so that quantum effects were ignorable, the average spin current exhibits bistability as a function of the laser that drives the cavity. We show that in the limit of a single quantum dot this bistability continues to be present in the intracavity photon statistics. Signatures of the bistable photon statistics manifest themselves in the frequency-dependent shot noise of the spin current despite the fact that the quantum-mechanical average spin current no longer exhibits bistability. Besides having significance for future quantum-dot-based optoelectronic devices, our results shed light on the relation between bistability, which is traditionally viewed as a classical effect, and quantum mechanics.

DOI: 10.1103/PhysRevB.78.195316 PACS number(s): 42.50.Pq, 73.63.Kv, 78.67.Hc

I. INTRODUCTION

Bistability is a phenomenon that readily occurs in classical systems that possess a nonlinear response to some input signal. In a bistable system the output function $F(I)$ can exhibit two stable states for a certain range of the input I such that when I is varied $F(I)$ follows a hysteresis loop. One of the most familiar examples is the hysteresis curve in the magnetization of a ferromagnetic material in the presence of an external magnetic field. In the context of electronics, digital flip-flop circuits and Schmitt triggers are common examples of bistable circuits. In nonlinear optics, optical bistability (OB) occurs in the input-output function of an optical resonator that contains a nonlinear dielectric and is driven by a laser.[1] OB has a number of applications in optical communications and computing not only because it can be used to build all optical switches, logic gates, and optically bistable memory devices[2–6] but it is also interesting for basic studies of phase transitions between stationary but nonequilibrium states.[3,7]

Here we explore a model[8] for a quantum dot (QD) "spin current battery" that unifies research in nonlinear quantum optics with spintronics. In the present work, we further develop that model to explore how bistability manifests itself in the quantum world. In our previous work,[9] we considered the classical limit of a large number of quantum dots, $N \gg 1$, interacting with a single optical microcavity mode such that all quantum-mechanical effects were ignorable. It was found that when the cavity is driven by a laser, the system exhibits classical absorptive OB in the amplitude of the cavity field. Because the spin current classically is a function of the cavity field amplitude, the spin current also exhibits bistability as a function of the amplitude of the driving laser which survives even in the presence of significant inhomogeneous variations in the dot sizes and coupling to the cavity field. However, this bistability is a purely classical effect since a large number of dots collectively interacts with the cavity mode like a single classical absorber. This begs the question of what happens if we consider only a *single* quantum dot coupled to the cavity where quantum fluctuations will be so large as to imply that the two "stable" outputs lose their stability. We show here that while the average spin current no longer exhibits any signature of bistability for a single dot the frequency-dependent spin current shot noise does reveal the underlying "stable values."

A spin current is defined as $I_s = s(I_\uparrow - I_\downarrow)$, which occurs when spin-up ($\uparrow$) and spin-down ($\downarrow$) charge carriers are moving in the opposite direction in contrast to the charge current $I_c = q(I_\uparrow + I_\downarrow)$, where they move in the same direction. Here, I_σ are the spin polarized particle currents, $s = \hbar/2$ is the spin of the particle, and $q = e$ is the charge. The interest in spin currents comes from spintronics, which has emerged as a field in which the spin degrees of freedom of charge carriers in solid-state devices are exploited for the purpose of information processing. Manipulation of the spin degrees of freedom rather than the charge has the advantage of longer coherence and relaxation times since the spin is more weakly coupled to its environment.[10] For the same reason, manipulation of the spin of an electron is much harder than the charge and therefore has resulted in significant effort to come up with proposals for necessary spin devices including spin batteries, spin filters, spin transistors, etc. There currently exist numerous theoretical and experimental concepts for generating spin currents in semiconductor nanostructures including spin-orbit (SO) interactions,[11,12] optical absorption,[13] and Raman scattering,[14] as well as various types of quantum pumps.[15–20] Electron-spin resonance (ESR) between Zeeman states in a quantum dot connected to leads is one of the proposed models for the generation of pure spin currents.[21,22] Our original model[8] extends the idea of ESR to spin flips induced by Raman transitions inside an optical microcavity. One laser involved in the Raman transition is a strong undepleted pump while the other is a mode of the cavity. Inside the cavity, both the feedback effect resulting from light "bouncing" back and forth numerous times in the cavity, which is the source of the bistability, as well as the quantum fluctua-

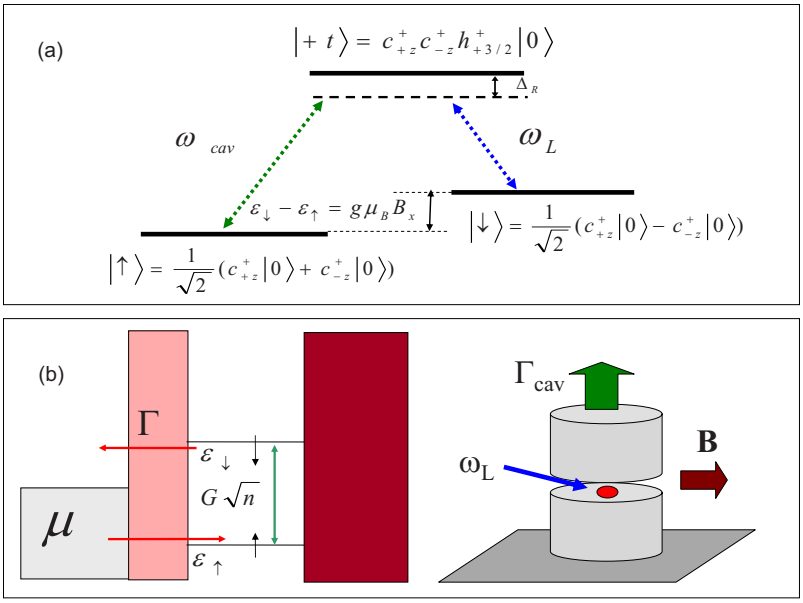

FIG. 1. (Color online) (a) Raman transition between the dot Zeeman states $|\uparrow,\downarrow\rangle$ via an intermediate trion state $|+t\rangle$ induced by a laser with frequency ω_L and a cavity mode with frequency ω_{cav}. Both optical fields are detuned from the trion energy by the amount Δ_R implying that $|+t\rangle$ is a virtual state. The spin eigenstates along the direction of the magnetic field are superpositions of spin eigenstates in the growth direction $\hat{c}^{\dagger}_{\pm z}|0\rangle$. (b) Schematic of a single quantum dot indicating Zeeman energy levels in the dot and allowed tunneling between the lead and dot. Also shown to the right is a hypothetical configuration of a dot in a micropillar cavity showing the direction of the magnetic field, pump laser, and cavity decay.

tions can have a dramatic influence on the characteristics of the spin current.

We would like to point out earlier theoretical work of a similar nature in quantum optics that explored the limit of "bistability" for a single atom coupled to cavity mode.[23–26] They found that steady-state pseudo-phase-space distribution of the cavity field had a bimodal structure indicative of two "stationary" values. These states are not however stable since quantum noise forces stochastic jumps between the two values.[25] Experiments have also shown that classical bistability only emerges when the number of atoms interacting with a cavity mode becomes much larger than 1.[27] The single-atom system is a significantly less rich physical system than our quantum dot model since there are no leads attached to an atom and hence no possibility of charge (or spin) current or, for that matter, current shot noise. In contrast to the mentioned work from quantum optics,[23–26] which relied on quantum trajectory Monte Carlo simulations, we utilize a standard master equation to calculate the shot noise.

In Sec. II, we briefly review our model and introduce our mathematical formulation of the shot noise in terms of the dot+cavity master equation. In Sec. III, we numerically study both the average spin current and the associated shot noise. In Sec. IV, we present our conclusions.

II. MODEL

We consider a self-assembled quantum dot embedded in a high-Q microcavity, as depicted in Fig. 1. We are interested in simultaneous coupling of a dot to a cavity mode and electrical transport through the dot due to tunneling from a doped reservoir. A number of experiments has already measured the conductance and shot noise through individual self-assembled quantum dots[28–31] as well as spectroscopy of exciton and charged exciton states in quantum dots with controllable charging from a doped lead.[32–34] Other experiments have demonstrated strong coupling of individual dots to a single optical microcavity mode.[35,36] Recently several of these directions have come together in the experiment by Strauf *et al.*[37] showing a high-efficiency single-photon quantum dot source. The experiment demonstrated electrical gate controlled charging of dot, which was embedded in a high-Q optical microcavity, from an n-doped layer. Several other experiments have followed demonstrating electrically driven quantum dots embedded in high-Q micropillar cavities that behave as single-photon sources.[38,39]

We assume that a single-electron reservoir at chemical potential μ is coupled to the dot via tunneling. Only a single empty orbital energy level ε of the dot lies close to μ. The Zeeman splitting between the two electron-spin states is $\Delta=\varepsilon_\downarrow-\varepsilon_\uparrow=g_x\mu_B B$, where B is a static magnetic field along the x axis that is perpendicular to the growth direction (z). μ_B is the Bohr magneton and g_x is the electronic g factor along the direction of the magnetic field. The energy levels satisfy $\varepsilon_\uparrow=\varepsilon-\Delta/2<\mu<\varepsilon_\downarrow=\varepsilon+\Delta/2$, so that only spin-up electrons can tunnel into the dot and only spin-down electrons can tunnel out. In the limit of very large Coulomb blockade energy, which we consider here, only a single electron from the reservoir can occupy the dot. The Zeeman states along the direction of the B field are superpositions of spin eigenstates along the growth direction $|\uparrow,\downarrow\rangle=(1/\sqrt{2})(\hat{c}^{\dagger}_{\uparrow z}|0\rangle\pm\hat{c}^{\dagger}_{\downarrow z}|0\rangle)$, where $\hat{c}^{\dagger}_{\sigma}$ is an electron creation operator.

Raman transitions between the dot Zeeman states $|\uparrow,\downarrow\rangle$ via an intermediate trion state $|+t\rangle$ are induced by a σ^+ polarized laser with frequency ω_L and a linearly polarized cavity mode with frequency ω_{cav}. Several experiments have already demonstrated the use of Raman scattering via an intermediate trion state to manipulate electron-spin states in quantum dots,[33,40–42] and theoretically such processes have been studied inside optical microcavities for use as a quantum computer.[43] The σ^+ pump creates a $+3/2$ heavy hole and an electron with spin down along the z direction according to the Hamiltonian $H_{\text{pump}}=(\hbar\Omega_l/2)\exp(-i\omega_l t)\hat{c}^{\dagger}_{\downarrow z}\hat{h}^{\dagger}_{+3/2}+\text{H.c.}$, which couples to the component of the dot Zeeman states with spin up along z yielding a trion state with an electron singlet. The σ^+ component of the cavity field along with the

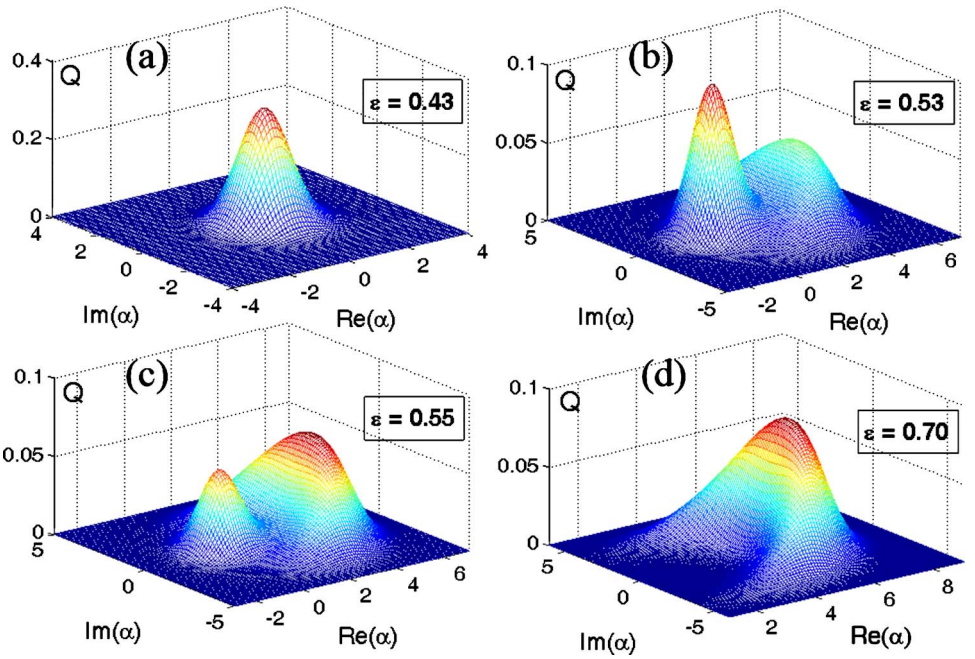

FIG. 2. (Color online) Q distribution vs Re[α] and Im[α] for $\Gamma_{\mathrm{cav}}=0.2\Gamma$, $g=2\Gamma$ and in clockwise order (a) $\epsilon=0.43\Gamma$, (b) 0.53Γ, (c) 0.55Γ, and (d) 0.7Γ.

pump leads to Raman transitions via the intermediate $|+t\rangle$ state that flips the electron spin while the σ^- component gives rise to additional energy shifts due to the ac Stark effect. When the two fields are far detuned by an amount Δ_R from the creation energy for the $|+t\rangle$ state, the intermediate trion state can be adiabatically eliminated to give $H_I=i\hbar g(\hat{a}\hat{c}_{\downarrow}^{\dagger}\hat{c}_{\uparrow}e^{i\omega_l t}-\mathrm{H.c.})$, where $g=g_{\mathrm{cav}}\Omega_l/4\Delta_R$ and $\hat{a}$ is the photon annihilation operator for the cavity mode.[8,9] We have absorbed all energy shifts of the states $|\sigma\rangle$ due to the ac Stark effect into a renormalization of the energy levels ε_σ. Nonresonant terms $\hat{a}^{\dagger}\hat{c}_{\downarrow}^{\dagger}\hat{c}_{\uparrow}e^{-i\omega_l t}+\mathrm{H.c.}$ can be neglected provided that $|\Delta-(\omega_{\mathrm{cav}}-\omega_l)|\ll|\Delta+(\omega_{\mathrm{cav}}-\omega_l)|$.

As one can see in Fig. 1, if an electron enters the dot in the spin $\uparrow$ state, a photon must be absorbed from the cavity mode and emitted into the pump in order to generate a spin current. It is therefore necessary to drive the cavity field. We assume that the cavity is driven by a classical source oscillating at frequency ω_p, $H_p=i\hbar\epsilon[\exp(-i\omega_p t)\hat{a}^{\dagger}-\mathrm{H.c.}]$, corresponding to coherent coupling between a laser and the cavity mode.[1,44]

The Hamiltonian in a frame rotating at the frequency ω_p is $H'=H_0'+H_P'+H_I'$,

$$H_0'=\hbar(\omega_{cav}-\omega_p)\hat{A}^{\dagger}\hat{A}+\varepsilon(\hat{C}_{\uparrow}^{\dagger}\hat{C}_{\uparrow}+\hat{C}_{\downarrow}^{\dagger}\hat{C}_{\downarrow})+(\Delta+\omega_l-\omega_p)(\hat{C}_{\downarrow}^{\dagger}\hat{C}_{\downarrow}-\hat{C}_{\uparrow}^{\dagger}\hat{C}_{\uparrow})/2, \quad (1)$$

$$H_I'+H_P'=i\hbar g(\hat{A}\hat{C}_{\downarrow}^{\dagger}\hat{C}_{\uparrow}-\mathrm{H.c.})+i\hbar\epsilon(\hat{A}^{\dagger}-\mathrm{H.c.}). \quad (2)$$

Here, we have defined operators in a rotating frame $\hat{a}=\hat{A}e^{i\omega_p t}$, $\hat{c}_{\uparrow}=\hat{C}_{\uparrow}\exp[-i(\omega_l-\omega_p)t/2]$, and $\hat{c}_{\downarrow}=\hat{C}_{\downarrow}\exp[i(\omega_l-\omega_p)t/2]$. In this work we assume that the resonance conditions $\omega_{\mathrm{cav}}=\omega_p$ and $\Delta=\omega_p-\omega_l$ are always satisfied, so that the final Hamiltonian of the system is $H'=\varepsilon(\hat{C}_{\uparrow}^{\dagger}\hat{C}_{\uparrow}+\hat{C}_{\downarrow}^{\dagger}\hat{C}_{\downarrow})+i\hbar g(\hat{A}\hat{C}_{\downarrow}^{\dagger}\hat{C}_{\uparrow}-\mathrm{H.c.})+i\hbar\epsilon(\hat{A}^{\dagger}-\mathrm{H.c.})$.

The dynamics of the system can be described in terms of the density operator ρ for the cavity plus dot. The master equation for ρ is given by

$$\dot{\rho}=-i[H',\rho]/\hbar-\Gamma_{\mathrm{cav}}(\hat{A}^{\dagger}\hat{A}\rho-2\hat{A}\rho\hat{A}^{\dagger}+\rho\hat{A}^{\dagger}\hat{A})/2+\dot{\rho}|_{\mathrm{lead}}. \quad (3)$$

The first term describes coherent dynamics of the coupled QD-cavity system, the second term represents the cavity decay,[1,44] and the third term describes QD-lead coupling. The lead-dot coupling is most easily expressed in terms of the matrix elements of the density operator $\rho_{\sigma,\sigma'}^{(n,m)}=\langle n,\sigma|\rho|\sigma',m\rangle$, where $|\sigma,n\rangle$ represents a state with n photons in the cavity and $\sigma=0,\uparrow,\downarrow$ corresponding to no electrons, one spin-up, or one spin-down electron, respectively. The specific forms of the master equations for the lead coupling are[8,22]

$$\dot{\rho}_{0,0}^{(n,m)}|_{\mathrm{lead}}=\Gamma^{(-)}\rho_{\downarrow,\downarrow}^{(n,m)}-\Gamma^{(+)}\rho_{0,0}^{(n,m)}, \quad (4)$$

$$\dot{\rho}_{\uparrow,\uparrow}^{(n,m)}|_{\mathrm{lead}}=\Gamma^{(+)}\rho_{0,0}^{(n,m)}, \quad (5)$$

$$\dot{\rho}_{\downarrow,\downarrow}^{(n,m)}|_{\mathrm{lead}}=-\Gamma^{(-)}\rho_{\downarrow,\downarrow}^{(n,m)}, \quad (6)$$

$$\dot{\rho}_{\uparrow,\downarrow}^{(n,m)}|_{\mathrm{lead}}=-\Gamma^{(-)}\rho_{\uparrow,\downarrow}^{(n,m)}/2. \quad (7)$$

Here, $\Gamma^{(-)}$ is the rate at which spin-down electrons tunnel out of the dot into lead and $\Gamma^{(+)}$ is the rate at which spin-up electrons tunnel into the dot. We assume that the tunneling between the lead and the dot is spin independent, $\Gamma^{(+)}=\Gamma^{(-)}=\Gamma$. We can rewrite Eq. (3) in matrix form

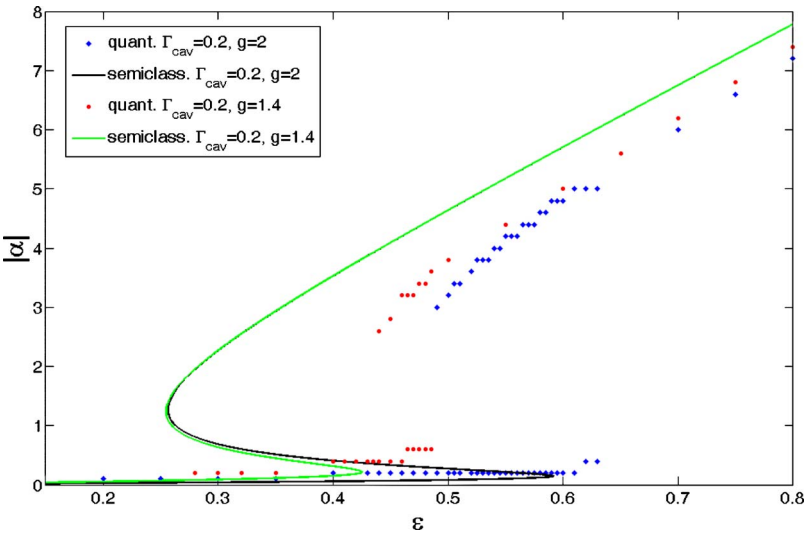

FIG. 3. (Color online) Peak values of the Q distribution as a function of ϵ (in units of Γ) for $\Gamma_{\mathrm{cav}}=0.2\Gamma$, $g=1.4\Gamma$ (circles) and $\Gamma_{\mathrm{cav}}=0.2\Gamma$, $g=2\Gamma$ (diamonds). For comparison, the classical solution (14) exhibiting bistability is also shown for the same parameters (green and black solid lines). One can see that the Q distribution for a single dot qualitatively follows the classical solution although the range of ϵ where bistability occurs is reduced by quantum fluctuations.

$$d\vec{\rho}/dt = M\vec{\rho}, \tag{8}$$

where $\rho^{(n,m)}_{\sigma_i,\sigma_i'} \rightarrow \vec{\rho}$ is the density matrix in vector form. The steady-state solution $\vec{\bar{\rho}}$ is given by the eigenvector of M with zero eigenvalue. Conservation of probability ensures that M has a zero eigenvalue.[45]

The spin current operator is defined as $\hat{I}_s = s(\hat{I}_\uparrow - \hat{I}_\downarrow)$ with the stationary currents given by $\langle \hat{I}_\uparrow \rangle = \Gamma \bar{\rho}_{0,0}$ and $\langle \hat{I}_\downarrow \rangle = -\Gamma \bar{\rho}_{\downarrow,\downarrow}$. Here $\bar{\rho}_{\sigma,\sigma'} = \Sigma_n \bar{\rho}^{(n,n)}_{\sigma,\sigma'}$ is the reduced density matrix of the dot after tracing over the cavity field and $s=\hbar/2$. We note that the spin current can be easily interpreted as the rate at which spin-up electrons tunnel into the empty dot, $\Gamma\bar{\rho}_{0,0}$, plus the rate at which spin-down electrons leave the dot, $-\Gamma\bar{\rho}_{\downarrow,\downarrow}$. The average spin current can be expressed in terms of expectation values of the cavity field using Eq. (3),

$$\langle I_s \rangle = 2s(2\epsilon\, \mathrm{Re}[\langle \hat{A} \rangle] - \Gamma_{\mathrm{cav}} \langle \hat{A}^\dagger \hat{A} \rangle). \tag{9}$$

One sees that the spin current is also the difference between the rate at which photons are coherently injected into the cavity by the driving laser, $2\epsilon\, \mathrm{Re}[\langle \hat{A} \rangle]$, and the rate at which photons decay from the cavity, $\Gamma_{\mathrm{cav}} \langle \hat{A}^\dagger \hat{A} \rangle$. Conservation of energy implies that this difference must be absorbed by a spin flip of the electron in the dot.

The noise power spectrum for the current can be expressed as the Fourier transform of the current-current correlation function

$$S_{\sigma,\sigma'}(\omega) = 2\int_{-\infty}^{\infty} dt\, e^{i\omega t} [\langle \hat{I}_\sigma(t) \hat{I}_{\sigma'}(0) \rangle - \langle \hat{I}_\sigma \rangle \langle \hat{I}_{\sigma'} \rangle]. \tag{10}$$

The spin current shot noise

$$S^{(s)} = 2\int_{-\infty}^{\infty} dt\, \exp(i\omega t) [\langle \hat{I}_s(t) \hat{I}_s(0) \rangle - \langle \hat{I}_s \rangle \langle \hat{I}_s \rangle]$$

can be written in terms of the shot-noise spectrum for the spin-resolved currents as $S^{(s)} = s^2(S_{\uparrow,\uparrow} + S_{\downarrow,\downarrow} - S_{\uparrow,\downarrow} - S_{\downarrow,\uparrow})$. It is well known that, for currents comprised of uncorrelated particles, the noise power spectrum is Poissonian; $S(\omega) = 2q\langle \hat{I} \rangle$, where q is the quantity transported by each particle in the current $\hat{I}$.[46] $q=e$ in the case of standard charge currents, while in our case the transported quantity is spin $q=s$. It is often convenient to measure the shot noise relative to the Poissonian noise by defining the Fano factor

$$F(\omega) = \frac{S^{(s)}(\omega)}{2sI_s}, \tag{11}$$

where I_s is the average spin current. $F(\omega) > 1$ represents super-Poissonian noise while $F(\omega) < 1$ represents sub-Poissonian noise.

Here we adopt the numerical method for evaluating Eq. (10) developed in Ref. 45 for use with master equations of the form (8). Briefly stated, the spectral decomposition of the matrix M is given by $M = \Sigma_\lambda \lambda \hat{P}_\lambda$, where λ is an eigenvalue of M and $\hat{P}_\lambda$ is the projection operator associated with that eigenvalue. This form of M can be used to evaluate the time evolution of the current operators $\hat{I}_\sigma$ and in the end yields the following form for the spin current shot noise:

$$S^{(s)}(\omega) = 2sI_s + 2\sum_{\lambda \neq 0} \left(\frac{\mathrm{Tr}[\hat{I}_s \hat{P}_\lambda \hat{I}_s \bar{\rho}]}{-i\omega - \lambda} + \frac{\mathrm{Tr}[\hat{I}_s \hat{P}_\lambda \hat{I}_s \bar{\rho}]}{i\omega - \lambda} \right). \tag{12}$$

The first term, the Poissonian contribution, is calculated from $I_s = \mathrm{Tr}[\hat{I}_s \bar{\rho}]$. Here we note that the projection operators can be calculated in terms of the left and right eigenvectors of M, $\hat{P}_\lambda = \vec{v}_\lambda (\vec{w}_\lambda)^\dagger$, where $(\vec{w}_\lambda)^\dagger M = \lambda (\vec{w}_\lambda)^\dagger$ define the left eigenvectors while $M\vec{v}_\lambda = \lambda \vec{v}_\lambda$ define the right eigenvectors. They satisfy the orthonormality relation $(\vec{w}_{\lambda_n})^\dagger \vec{v}_{\lambda_m} = \delta_{n,m}$. We note that this is a different formulation of the projection operators than what appears in Ref. 45 where $\hat{P}_\lambda = SE_nS^{-1}$, with S being the matrix whose columns are the right eigenvectors of M and E_n is a square matrix that has zero entries everywhere except the (n,n) element, which is 1. However, it is easy to show that these forms are mathematically equivalent.

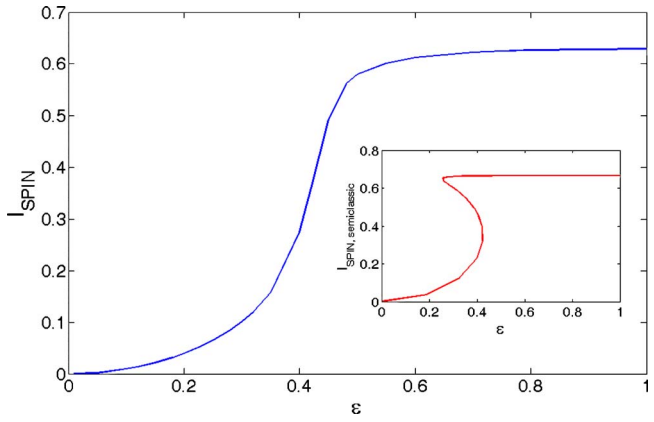

FIG. 4. (Color online) Average value of the spin current I_s (in units of $s\Gamma$) as a function of ϵ (in units of Γ) for $\Gamma_{cav}=0.2\Gamma$, $g=1.4\Gamma$. Inset shows the classical spin current obtained from Eq. (14) and $I_S=2s(2|\alpha||\epsilon|-\Gamma_{cav}|\alpha|^2)$. One can see that when quantum fluctuations are included, all indications of bistability are destroyed in the average current.

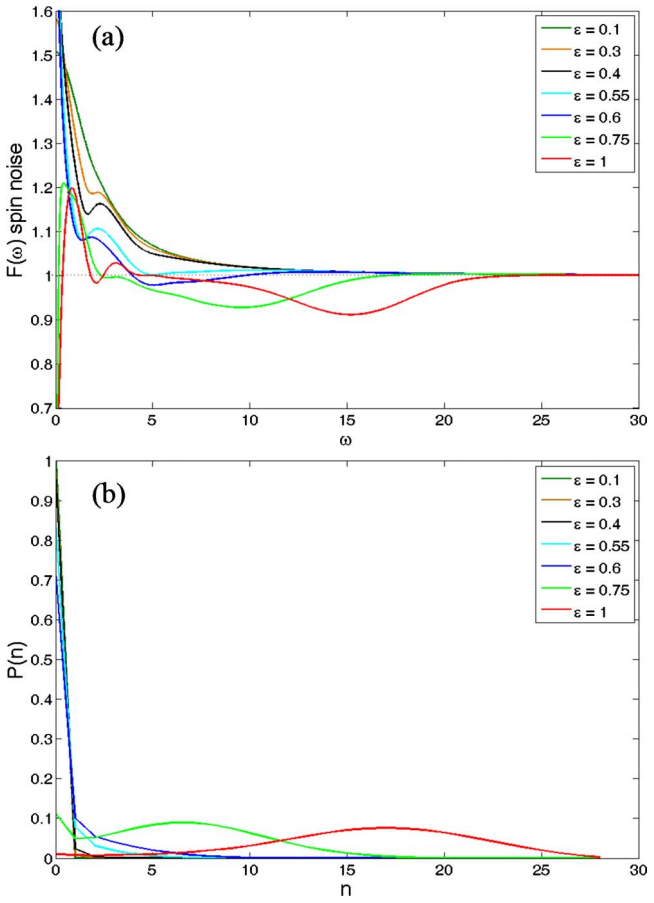

FIG. 5. (Color online) (a) Fano factor $F(\omega)$ for $\Gamma_{cav}=0.4\Gamma$, $g=2\Gamma$ and different values of ϵ (in units of Γ). (b) Steady-state probability distribution for photons in the cavity for the same parameters as in (a). Note that ω is measured in units of Γ.

Finally we note that in order to numerically solve Eq. (8) or Eq. (12), one must choose a maximum number of cavity photons N_{max} at which to truncate the density-matrix equations. This system is very sensitive to the cutoff since a too small N_{max} can lead to the artificial build up of populated photon states close to the cutoff that gives the appearance of bistability when in fact this is only a numerical artifact. For this reason, all simulations presented here used values of $N_{max}=40-120$ that were chosen to be sufficiently large so as to ensure that the results were insensitive to the particular choice of N_{max}. By contrast, we note that Figs. 2 and 3 in Ref. 9 are incorrect since the value of N_{max} was unknowingly chosen too small, namely, 20.

III. RESULTS

Our goal here is to analyze numerically the fully quantum behavior for a single quantum dot in the parameter regime where bistability is expected to occur. In doing so we will compare these results to the classical theory of bistability for $N\gg 1$ quantum dots developed in Ref. 9. By contrast to Ref. 9, where only the classical average spin current was studied, here we also focus our attention on the shot noise as a means to reveal bistability in the quantum limit.

We first discuss the behavior of the intracavity field as a function of the driving field amplitude ϵ. The intracavity field can be readily visualized in term of the Q distribution[1,44] for the cavity mode in the steady state as shown in Fig. 2. The Q distribution is defined as

$$Q(\alpha)=\sum_{\sigma=0,\uparrow,\downarrow}\langle\alpha,\sigma|\bar{\rho}|\alpha,\sigma\rangle/\pi,$$

where $|\alpha\rangle$ is a coherent state $\hat{A}|\alpha\rangle=\alpha|\alpha\rangle$. It represents a pseudo-quantum-mechanical phase-space distribution for bosonic quantum fields where $\mathrm{Re}[\alpha]$ and $\mathrm{Im}[\alpha]$, which represent the quadrature components of the field, can be interpreted as the position and momentum, respectively, of a fictitious particle. We note that there exists a number of different pseudo-phase-space distributions for bosonic fields whose utility depends on the particular problem.[44] We chose the Q distribution because it is both positive semidefinite and can also be interpreted as a probability distribution, namely, the probability of measuring the field in the coherent state $|\alpha\rangle$. This therefore allows qualitative comparisons to classical phase-space probability distributions.

In Fig. 2(a), which corresponds to weak driving, there is only single peak around $\alpha\approx 0$. This represents a cavity that is overdamped such that all energy injected into the cavity is absorbed by the dot. For larger driving, as in Figs. 2(b) and 2(c), there are two peaks: one at $\alpha\approx 0$ and another at $\mathrm{Re}[\alpha]>0$ and $\mathrm{Im}[\alpha]=0$. This represents the bistable situation where the cavity field has two most probable states. By contrast, in Fig. 2(d) one can see that the peak around $\alpha=0$ has completely disappeared and only a peak with $\mathrm{Re}[\alpha]>0$ remains when the driving is further increased. This peak corresponds to the case where the cavity driving is so strong that the dot transition is saturated. For a saturated transition, $\bar{\rho}_{0,0}=\bar{\rho}_{\uparrow,\uparrow}=\bar{\rho}_{\downarrow,\downarrow}=1/3$ such that the current obtains the maximum value, $\langle I_S\rangle=s(\Gamma\bar{\rho}_{0,0}+\Gamma\bar{\rho}_{\downarrow,\downarrow})=2s\Gamma/3$. Based on Eq. (9), the approximate location of this second peak in the Q distribution is then

$$|\alpha| = \frac{(2\epsilon/\Gamma_{cav}) + \sqrt{(2\epsilon/\Gamma_{cav})^2 - 4\Gamma/3\Gamma_{cav}}}{2}, \tag{13}$$

where we note that the last term due to the lead, $4\Gamma/3\Gamma_{cav}$, reduces the cavity field amplitude below the value of an empty cavity (i.e., no absorber in the cavity), $2\epsilon/\Gamma_{cav}$. Figure 3 shows the peak values of the Q distribution as a function of ϵ where one can see that a classic hysteresis loop emerges. This can be compared to the classical solution for the cavity amplitude that ignores quantum fluctuations,[9]

$$|\epsilon| - \Gamma_{cav}|\alpha|/2 = \frac{g^2|\alpha|\Gamma}{6g^2|\alpha|^2 + \Gamma^2/2}. \tag{14}$$

Equation (14) is obtained from the equations of motion for the expectation values of the cavity and dot operators by factorizing the expectation values of products of operators such as $\langle \hat{A}^\dagger \hat{C}_\uparrow^\dagger \hat{C}_\downarrow \rangle \rightarrow \langle \hat{A}^\dagger \rangle \langle \hat{C}_\uparrow^\dagger \hat{C}_\downarrow \rangle$ [Note that one recovers Eq. (13) from Eq. (14) in the limit that $g|\alpha| \gg \Gamma$]. One can see in Fig. 3 that in the quantum case, the range of ϵ values where bistability is present has been shifted to higher values due to quantum fluctuations.

By contrast, in Fig. 4, we present the quantum-mechanical average spin current for a single dot as a function of the driving amplitude. As one can see it is a single-valued quantity that shows no sign of the "switch back" behavior characteristic of bistability that is seen in the inset, which is the classical spin current calculated using Eq. (14) and $I_S = 2s(2|\alpha||\epsilon| - \Gamma_{cav}|\alpha|^2)$. In fact, the current is qualitatively the same as that calculated for spin flips in the case of ESR using a classical magnetic field.[22] This is not surprising since one can see from Eq. (9) that the spin current is the quantum-mechanical expectation value of the cavity field and despite the bimodal distribution of $Q(\alpha)$, the spin current is averaged over both values; $\langle I_S \rangle \approx P_1 I_{S,1} + P_2 I_{S,2}$, where P_j are the total probabilities corresponding to each of the two peaks in $Q(\alpha)$ and $I_{S,j} = 2s(2\epsilon \mathrm{Re}[\alpha_j] - \Gamma_{cav}\alpha_j^* \alpha_j)$, where α_j are the locations of the two peaks.

This begs the question, how does the bistable structure of the intracavity field manifest itself in quantum-mechanical observables? Previous work on the quantum limit of bistability for single-atom cavity QED focused on the quantum dynamics using "quantum trajectories" Monte Carlo simulations approach based on stochastic Schrödinger equations[23] and stochastic master equations,[25,26] which showed that the cavity field and photocurrent from the cavity undergo stochastic jumps between the two states given by the peaks in the Q distribution. In these systems, the average time between switching events was proportional to the spontaneous emission lifetime since it was the "wave-function collapse" due to spontaneous emission of the atom that drove the system between the two states.[25]

Equations (4)–(7) have a similar form to that of the master equation for atomic decay. Therefore we can draw an analogy with earlier work and argue that wave-function collapse resulting from electron-tunneling events into and out of the dot will induce jumps between the two stable quantum states of the cavity field. Since the time scale that determines transport through the dot is determined by the time needed for a spin flip, which is the Rabi frequency $g\sqrt{n}$, different cavity field states will result in different time intervals between successive electrons being "emitted" by the dot. One would therefore expect that the Rabi frequencies associated with the two stable field states would manifest themselves in the current-current correlations $\langle \hat{I}(t+\tau)\hat{I}(t) \rangle$.

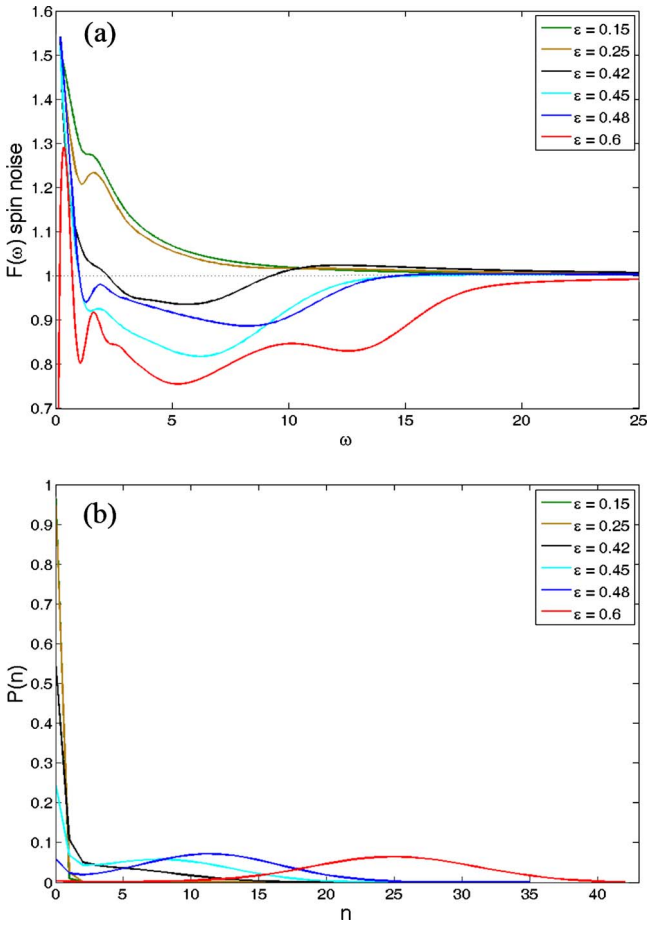

FIG. 6. (Color online) (a) Fano factor $F(\omega)$ for $\Gamma_{cav} = 0.2\Gamma$, $g = 1.4\Gamma$ and different values of ϵ (in units of Γ). (b) Steady-state probability distribution for photons in the cavity for the same parameters as in (a). Note that ω is measured in units of Γ.

Figures 5 and 6 show $F(\omega)$ and $P(n)$, the probability distribution for the cavity photons, for different values of ϵ. For the sake of comparison, Fig. 7 shows the Fano factor for the case of ESR, $F_{ESR}(\omega)$, with a classical field of Rabi frequency R that flips the spins of the electrons.[22] The classical field ESR Hamiltonian can be obtained by replacing $\hat{A}$ and $\hat{A}^\dagger$ with a c number ($\hat{A} \rightarrow \alpha$) in H' with $R = g\alpha$. We must emphasize that in this model of ESR in a quantum dot,[21,22] there is no cavity and as a result the field that flips the spin is simply an external parameter rather than a dynamic variable. Since it is the feedback effect of the cavity that induces bistability, bistability does not occur in ESR.

The similarity between Eqs. (4)–(7) and that of spontaneous emission allows us to define the critical dot number $N_0 = 2\Gamma\Gamma_{cav}/g^2$, which represents in the classical theory the minimum number of dots necessary for bistability to be present,[9,23] as well as the critical photon number n_c

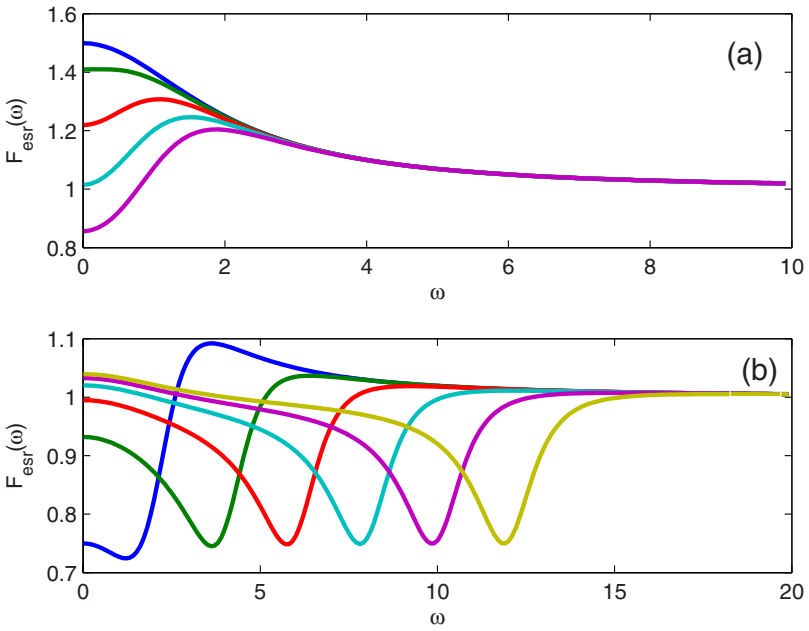

FIG. 7. (Color online) Fano factor $F_{\mathrm{ESR}}(\omega)$ for electron-spin resonance with a classical field of Rabi frequency R that flips the spins of the electrons. The zero-frequency Fano factor is given analytically by $F_{\mathrm{ESR}}(0)=\frac{3\Gamma^4+2\Gamma^2R^2+19R^4}{2(\Gamma^2+3R^2)^2}$. The frequency ω is in units of Γ and for (a) from top to bottom $R/\Gamma=0$, 0.1, 0.2, 0.3, and 0.4 are plotted while for (b) in order of the minima going from left to right $R/\Gamma=1$, 2, 3, 4, 5, and 6. As in the previous graphs, ω is in units of Γ.

$=\Gamma^2/4g^2$, which defines the number of photons necessary to significantly modify the dot response.[23] Classical bistability is predicted to occur in the limit $n_c\to\infty$ and therefore larger values of n_c should produce more pronounced bistability in the single-dot or -atom case.[24] For both Figs. 5 and 6 $N_0\approx 0.2$ while for Fig. 5 $n_c=0.063$ and for Fig. 6 $n_c=0.13$. This behavior with n_c is confirmed in the figures where the bimodality of $P(n)$ is more visible and present for a larger range of values in Fig. 6 as compared to Fig. 5.

In these figures, we can see that for small ϵ, below the threshold for the onset of bistability, $F(\omega)$ is super-Poissonian for low frequencies and Poissonian at high frequencies, which is similar to the case of ESR for small R where $F_{\mathrm{ESR}}(0)\to 3/2$ for $R\to 0$. For small ϵ, the cavity is overdamped and only the vacuum state has significant probability $P(0)$, and therefore transitions are primarily driven by fluctuations above the vacuum state. In the opposite extreme with stronger ϵ in the bistability region, which is most clearly seen in Fig. 6 for $\epsilon/\Gamma=0.42, 0.45, 0.48$, $F(\omega)$ remains super-Poissonian at zero frequency while at $\omega\approx 2g|\alpha_2|$ a broad sub-Poissonian dip develops whose overall width is determined by the width of $P(n)$ around the second maximum at $n_2=|\alpha_2|^2$. This behavior is a mixture of the ESR system for small and large R since as already mentioned, F_{ESR} is super-Poissonian at low frequencies $R\ll\Gamma$. By contrast, the ESR system exhibits a sub-Poissonian dip at $2R$ for $R>\Gamma$ while being nearly Poissonian at zero frequency $[F_{\mathrm{ESR}}(0)\to 19/18$ for $R\to\infty]$. For even larger ϵ such as $\epsilon/\Gamma=1$ in Fig. 5 or $\epsilon/\Gamma=0.6$ in Fig. 6, which places the system outside the bistable regime, one can see that the broad sub-Poissonian dip around $\omega\approx 2g|\alpha_2|$ persists but that $F(0)$ is no longer super-Poissonian but rather has become sub-Poissonian. Therefore we can conclude that the super-Poissonian behavior of $F(0)$ is attributable to the maximum in $P(n)$ at $n=0$ while the sub-Poissonian dip is attributable to the maximum in $P(n)$ around $|\alpha_2|^2$.

IV. CONCLUSIONS

Here we have analyzed the spin current and shot noise from a single quantum dot embedded inside a driven optical microcavity. We have shown that as a result of the cavity-field-induced spin flips, the quantum bistability present in the cavity field Q distribution manifests itself also in the spin current shot noise from the dot. These results indicate that despite the large quantum fluctuations that wipe out all trace of the bistability in the average current, the shot noise reveals the underlying bimodal distribution of the cavity field. This works implies that there is no need to make recourse to more complicated methods such as stochastic wave-function methods in order to detect bistability in the presence of large quantum fluctuations.

ACKNOWLEDGMENT

This work was supported by the National Science Foundation.

[1] P. Meystre and M. Sargent III, *Elements of Quantum Optics*, 3rd ed. (Springer-Verlag, Berlin, 1998).
[2] A. Miller, D. A. B. Miller, and S. D. Smith, Adv. Phys. **30**, 697 (1981).
[3] E. Abraham and S. D. Smith, Rep. Prog. Phys. **45**, 815 (1982).
[4] H. M. Gibbs, *Optical Bistability: Controlling Light with Light* (Academic, New York, 1985).
[5] P. Mandel, S. D. Smith, and B. S. Wherrett, *From Optical Bista-*

bility Towards Optical Computing (North-Holland, Amsterdam, 1987).
[6] M. E. Warren, S. W. Koch, and H. M. Gibbs, Computer **20**, 68 (1987).
[7] R. Bonifacio and L. A. Lugiato, Opt. Commun. **19**, 172 (1976).
[8] I. Djuric and C. P. Search, Phys. Rev. B **74**, 115327 (2006).
[9] I. Djuric and C. P. Search, Phys. Rev. B **75**, 155307 (2007).
[10] Igor Žutić, Jaroslav Fabian, and S. Das Sarma, Rev. Mod. Phys. **76**, 323 (2004).
[11] M. I. D'yakonov and V. I. Perel', JETP Lett. **13**, 467 (1971); J. E. Hirsch, Phys. Rev. Lett. **83**, 1834 (1999); S. Zhang, *ibid.* **85**, 393 (2000); T. P. Pareek, *ibid.* **92**, 076601 (2004).
[12] E. I. Rashba, Physica E (Amsterdam) **20**, 189 (2004).
[13] Martin J. Stevens, Arthur L. Smirl, R. D. R. Bhat, Ali Najmaie, J. E. Sipe, and H. M. van Driel, Phys. Rev. Lett. **90**, 136603 (2003); R. D. R. Bhat and J. E. Sipe, *ibid.* **85**, 5432 (2000).
[14] A. Najmaie, E. Ya. Sherman, and J. E. Sipe, Phys. Rev. Lett. **95**, 056601 (2005).
[15] E. R. Mucciolo, C. Chamon, and C. M. Marcus, Phys. Rev. Lett. **89**, 146802 (2002).
[16] Susan K. Watson, R. M. Potok, C. M. Marcus, and V. Umansky, Phys. Rev. Lett. **91**, 258301 (2003).
[17] P. Sharma and C. Chamon, Phys. Rev. Lett. **87**, 096401 (2001); R. Citro, N. Andrei, and Q. Niu, Phys. Rev. B **68**, 165312 (2003).
[18] R. Benjamin and C. Benjamin, Phys. Rev. B **69**, 085318 (2004).
[19] M. Blaauboer and C. M. L. Fricot, Phys. Rev. B **71**, 041303(R) (2005).
[20] E. Sela and Y. Oreg, Phys. Rev. B **71**, 075322 (2005).
[21] B. Wang, J. Wang, and H. Guo, Phys. Rev. B **67**, 092408 (2003); P. Zhang, Qi-Kun Xue, and X. C. Xie, Phys. Rev. Lett. **91**, 196602 (2003).
[22] Bing Dong, H. L. Cui, and X. L. Lei, Phys. Rev. Lett. **94**, 066601 (2005).
[23] M. A. Armen and H. Mabuchi, Phys. Rev. A **73**, 063801 (2006).
[24] C. M. Savage and H. J. Carmichael, IEEE J. Quantum Electron. **24**, 1495 (1988).
[25] P. Alsing and H. J. Carmichael, Quantum Opt. **3**, 13 (1991).
[26] H. Mabuchi and H. M. Wiseman, Phys. Rev. Lett. **81**, 4620 (1998).
[27] G. Rempe, R. J. Thompson, R. J. Brecha, W. D. Lee, and H. J. Kimble, Phys. Rev. Lett. **67**, 1727 (1991).
[28] K. H. Schmidt, M. Versen, U. Kunze, D. Reuter, and A. D. Wieck, Phys. Rev. B **62**, 15879 (2000).
[29] T. Ota, K. Ono, M. Stopa, T. Hatano, S. Tarucha, H. Z. Song, Y. Nakata, T. Miyazawa, T. Ohshima, and N. Yokoyama, Phys. Rev. Lett. **93**, 066801 (2004).
[30] P. Barthold, F. Hohls, N. Maire, K. Pierz, and R. J. Haug, Phys. Rev. Lett. **96**, 246804 (2006).
[31] G. Kießlich, A. Wacker, E. Schöll, S. A. Vitusevich, A. E. Belyaev, S. V. Danylyuk, A. Förster, N. Klein, and M. Henini, Phys. Rev. B **68**, 125331 (2003).
[32] D. Heiss, M. Kroutvar, J. J. Finley, and G. Abstreiter, Solid State Commun. **135**, 591 (2005).
[33] Mete Atatüre, Jan Dreiser, Antonio Badolato, Alexander Högele, Khaled Karrai, and Atac Imamoglu, Science **312**, 551 (2006).
[34] R. J. Warburton, C. Schaflein, D. Haft, F. Bickel, A. Lorke, K. Karrai, J. M. Garcia, W. Schonfeld, and P. M. Petroff, Nature (London) **405**, 926 (2000).
[35] J. P. Reithmaier, G. Sęk, A. Löffler, C. Hofmann, S. Kuhn, S. Reitzenstein, L. V. Keldysh, V. D. Kulakovskii, T. L. Reinecke, and A. Forchel, Nature (London) **432**, 197 (2004); T. Yoshie, A. Scherer, J. Hendrickson, G. Khitrova, H. M. Gibbs, G. Rupper, C. Ell, O. B. Shchekin, and D. G. Deppe, *ibid.* **432**, 200 (2004).
[36] E. Peter, P. Senellart, D. Martrou, A. Lemaître, J. Hours, J. M. Gérard, and J. Bloch, Phys. Rev. Lett. **95**, 067401 (2005).
[37] S. Strauf, N. G. Stoltz, M. T. Rakher, L. A. Coldren, P. M. Petroff, and D. Bouwmeester, Nat. Photonics **1**, 704 (2007).
[38] C. Bockler, S. Reitzenstein, C. Kistner, R. Debusmann, A. Loffler, T. Kida, S. Hofling, A. Forchel, L. Grenouillet, J. Claudon, and J. M. Gerard, Appl. Phys. Lett. **92**, 091107 (2008).
[39] D. J. P. Ellis, A. J. Bennett, S. J. Dewhurst, C. A. Nicoll, D. A. Ritchie, and A. J. Sheilds, New J. Phys. **10**, 043035 (2008).
[40] P. Chen, C. Piermarocchi, L. J. Sham, D. Gammon, and D. G. Steel, Phys. Rev. B **69**, 075320 (2004).
[41] A. Greilich, R. Oulton, E. A. Zhukov, I. A. Yugova, D. R. Yakovlev, M. Bayer, A. Shabaev, A. L. Efros, I. A. Merkulov, V. Stavarache, D. Reuter, and A. Wieck, Phys. Rev. Lett. **96**, 227401 (2006).
[42] M. V. Gurudev Dutt, J. Cheng, B. Li, X. Xu, X. Li, P. R. Berman, D. G. Steel, A. S. Bracker, D. Gammon, S. E. Economou, R.-B. Liu, and L. J. Sham, Phys. Rev. Lett. **94**, 227403 (2005).
[43] A. Imamoglu, D. D. Awschalom, G. Burkard, D. P. DiVincenzo, D. Loss, M. Sherwin, and A. Small, Phys. Rev. Lett. **83**, 4204 (1999).
[44] D. F. Walls and G. J. Milburn, *Quantum Optics* (Springer-Verlag, Berlin, 1994).
[45] I. Djuric, B. Dong, and H. L. Cui, J. Appl. Phys. **99**, 063710 (2006).
[46] Y. M. Blanter and M. Büttiker, Phys. Rep. **336**, 1 (2000); C. Beenakker and C. Schönenberger, Phys. Today **56** (5), 37 (2003).